EM Implosion Memos

Memo 7

Nov 2006

Numerical Calculation for the Waveforms Near the Second Focus of a Prolate-Spheroidal IRA

Serhat Altunc, Carl E. Baum and Christos Christodoulou

University of New Mexico
Department of Electrical and Computer Engineering
Albuquerque New Mexico 87131

Abstract

This paper focus on the numerical results for the waveforms near the second focus of a prolate-spheroidal IRA. Both numerical and analytical calculations are for IRAs with different feed arms. Variations of the waveforms for x, y and z-axis variations near the second focus are found for 2-TEM-feed-arm, 45^{o} 4-TEM-Feed-Arm and 60^{o} 4-TEM-Feed-Arm cases are calculated and compared.

1 Introduction

This paper is a numerical calculation of a prolate-spheroidal IRA that is based on [1],[2],[3]. The waveforms for 2-TEM-Feed-Arm, 45^{o} 4-TEM-Feed-Arm and 60^{o} 4-TEM-Feed-Arm cases for x, y, z axis variations near the second focus are calculated.

1.1 Description of geometry

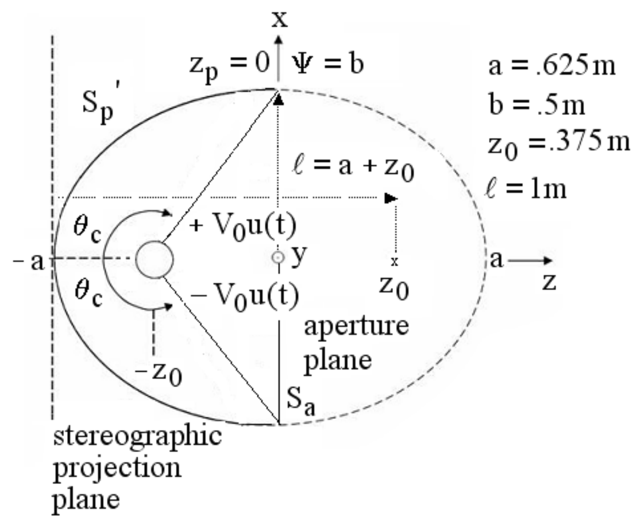

Figure 1.1 IRA Geometry

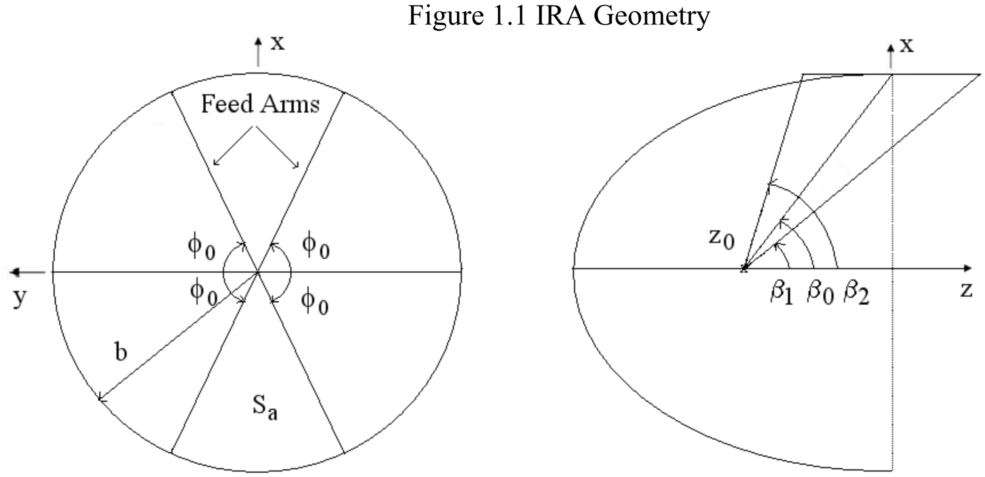

Figure 1.2 Feed Arm Geometry

For our design, we choose a special case of the prolate-spheroidal IRA's geometric parameters as [3]

$$z_p = 0,\ b = \Psi_0 = .5\text{m},\ a = .625\text{ m},\ z_0 = .375\text{m},\ \ell = 1\text{m} \tag{1.1}$$

ϕ_o is the angle from y-axis to the feed arm and $\beta_0, \beta_1, \beta_2$ are the angles from the z-axis to the electrical center, the first edge and the second edge of the feed arms as in Fig. 1.2

2 Analytical Focal Waveforms and Spot Sizes

2.1 Analytical focal waveforms

The analytical focal waveforms are from [1,2]. The excitation is a 1 Volt ($V_0 = .5$ Volt) step, rising as a ramp function lasting 100 ps.

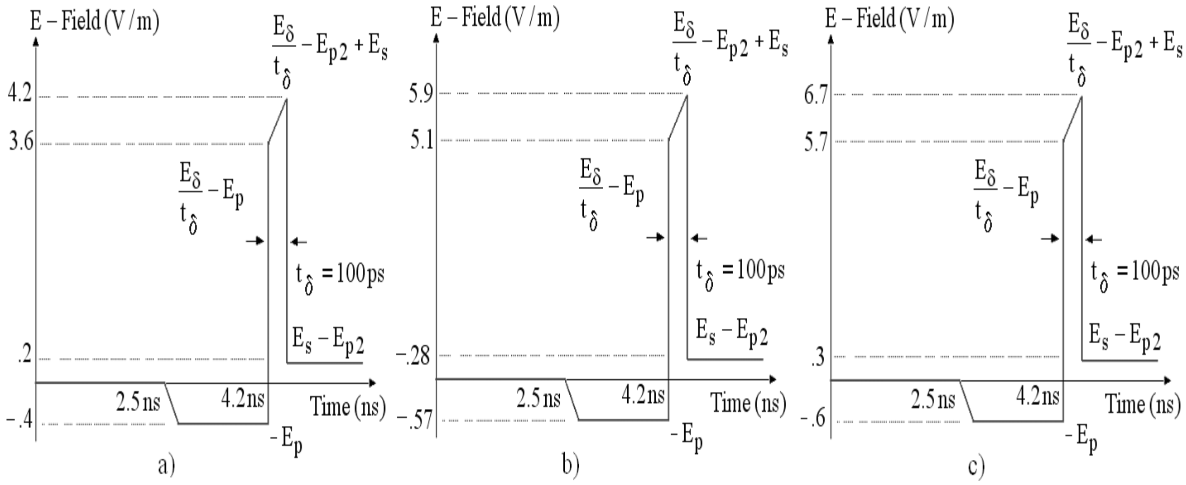

Figure 2.1 Analytical Focal Waveforms a) 2-Arm $400\,\Omega$ b) 45^0 degree 4-Arm $200\,\Omega$ c) 60^0 degree 4-Arm $200\,\Omega$

2.2 Spot sizes

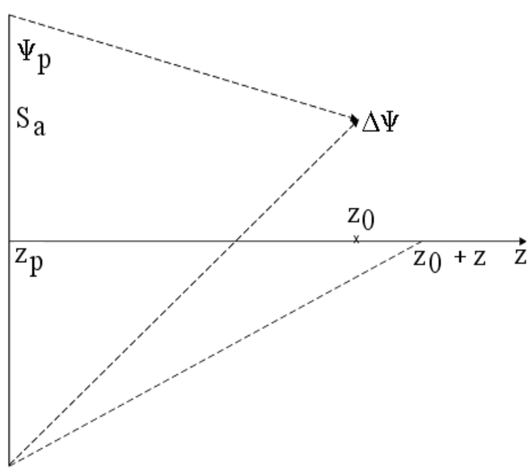

Figure 2.2 Dispersion of Impulse Near z_0

Given that the impulse has some small width $t_\delta = 100$ ps, the maximum fields will exist in some small region around z_0. We can make a rough estimate of spot sizes [3] as follows

Pulse width to define boundary spot with respect to Ψ and z

$$t_\Psi = t_z = 2t_\delta = 200\,\text{ps} \tag{1.2}$$

So spot sizes from (6.8) in [3] are

$$|\Delta z| = 2\,[1 - z_0 / a]^{-1} c t_\delta = 15\,\mathrm{cm}$$
$$\Delta\Psi = \frac{a}{b} c t_\delta = 3.75\,\mathrm{cm} \tag{1.3}$$

These calculations are based on the 2-arm case. It is the same as the 45^{o} 4-Arm case except for a factor of $\sqrt{2}$. This does not apply to the 60^{o} 4-Arm case. So we are trying to find spot sizes for the 60^{o} case from our numerical results.

3 Numerical Waveforms

3.1 Numerical waveforms for 2-TEM-feed-arms

3.1.1 Numerical waveforms wrt x-axis variations for 2-TEM-feed-arms

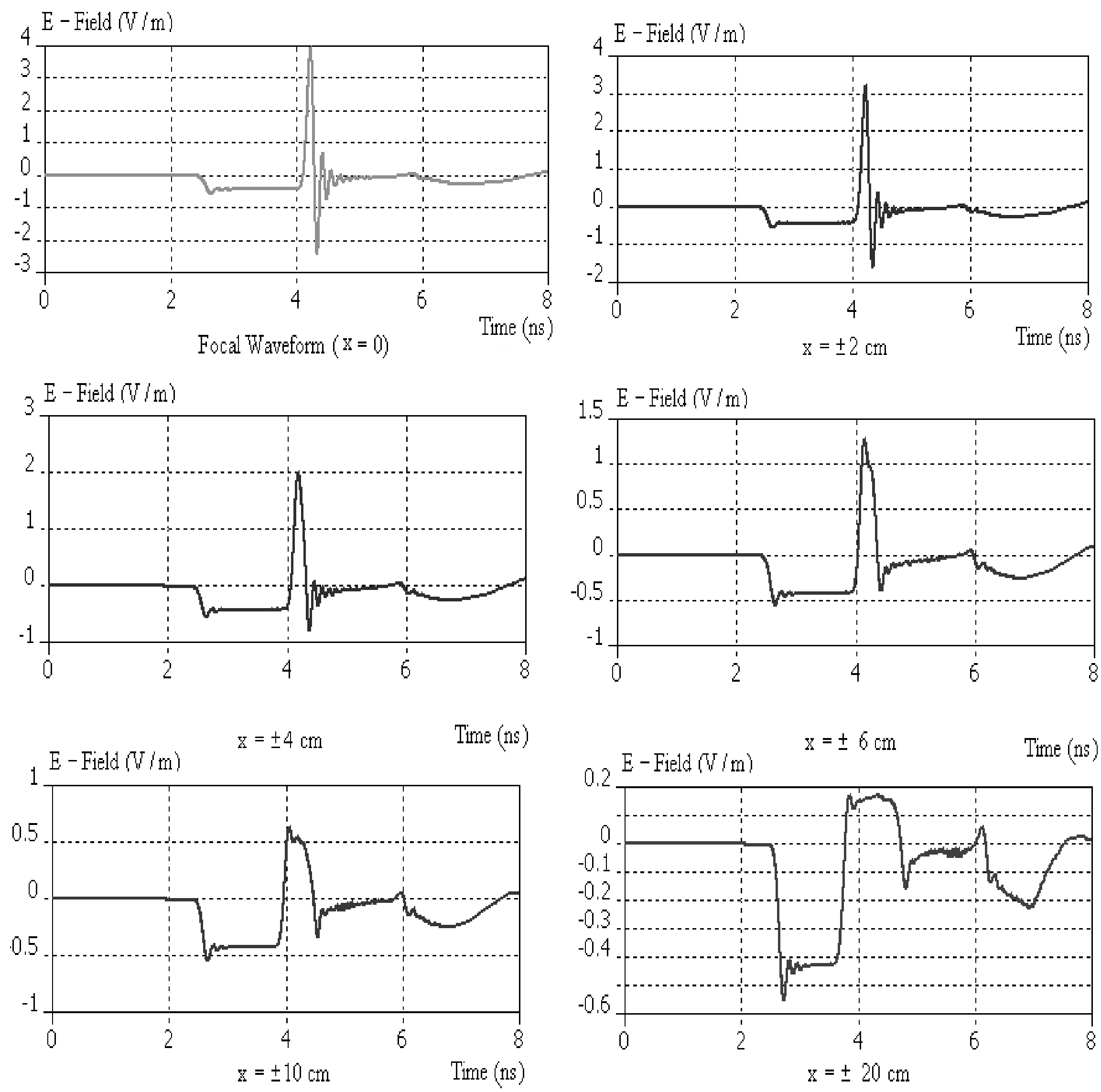

Figure 3.1 Numerical Waveforms wrt x-axis Variations

$x = 0$ is one of the symmetry planes of our design. One can see from Fig. 3.1 at $x = \pm 4\,cm$ the waveform starts to disperse as expected from (1.3).

3.1.2 Numerical waveforms wrt y-axis variations for 2-TEM-feed-arms

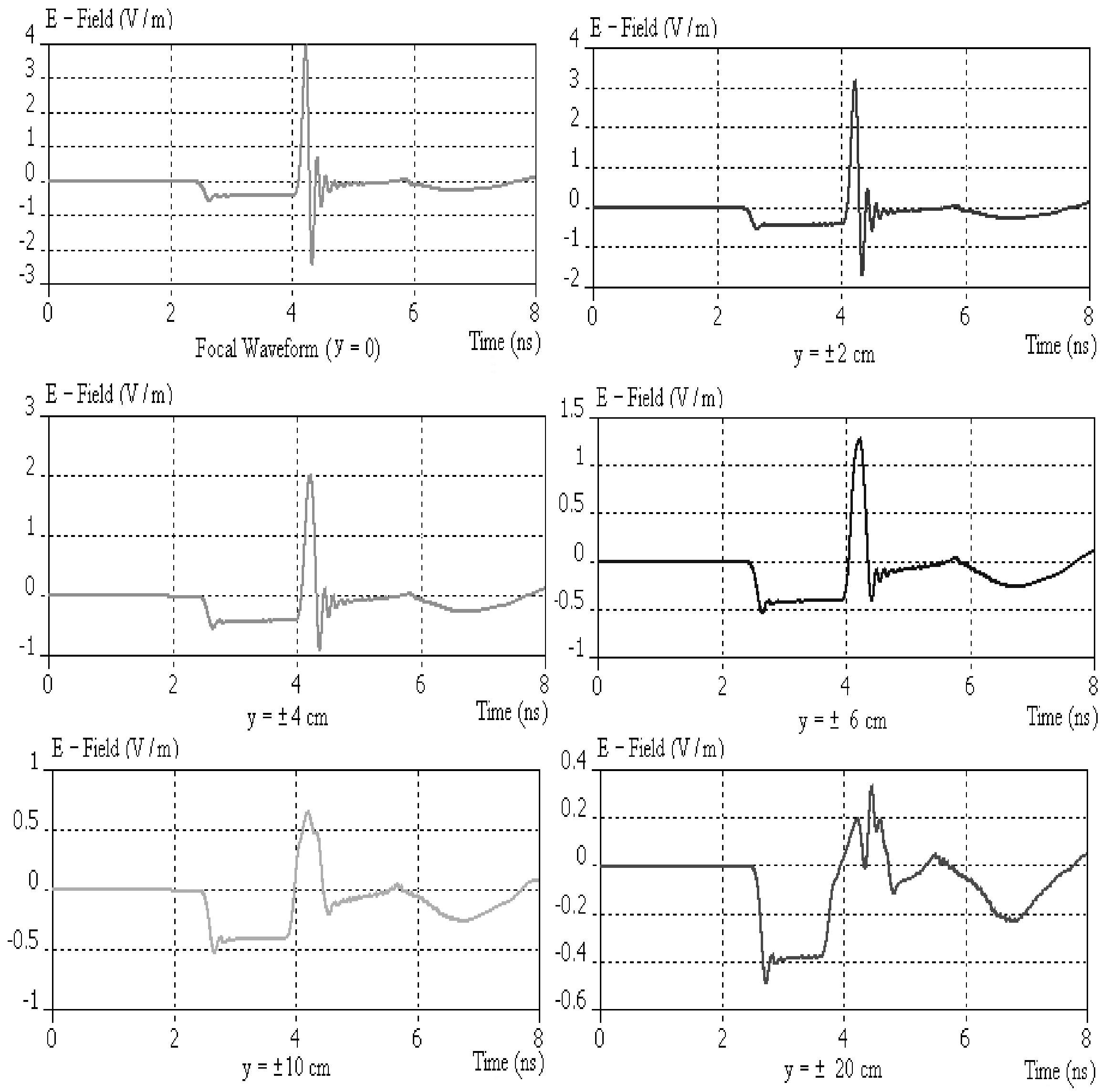

Figure 3.2 Numerical Waveforms wrt y-axis Variations

$y = 0$ is one of the symmetry planes of our design. We start to see dispersion at $y = \pm 4\,cm$. If we compare the waveform for $x = \pm 4\,cm$ and $y = \pm 4\,cm$, we can see that we have a higher amplitude for x- axis variation. It is expected because if we move along the y-axis we are away from the feed arms. But for the x-axis we are getting closer to one feed arm while we are getting far away from the other one.

3.1.3 Numerical waveforms wrt z-axis variations for 2-TEM-feed-arms

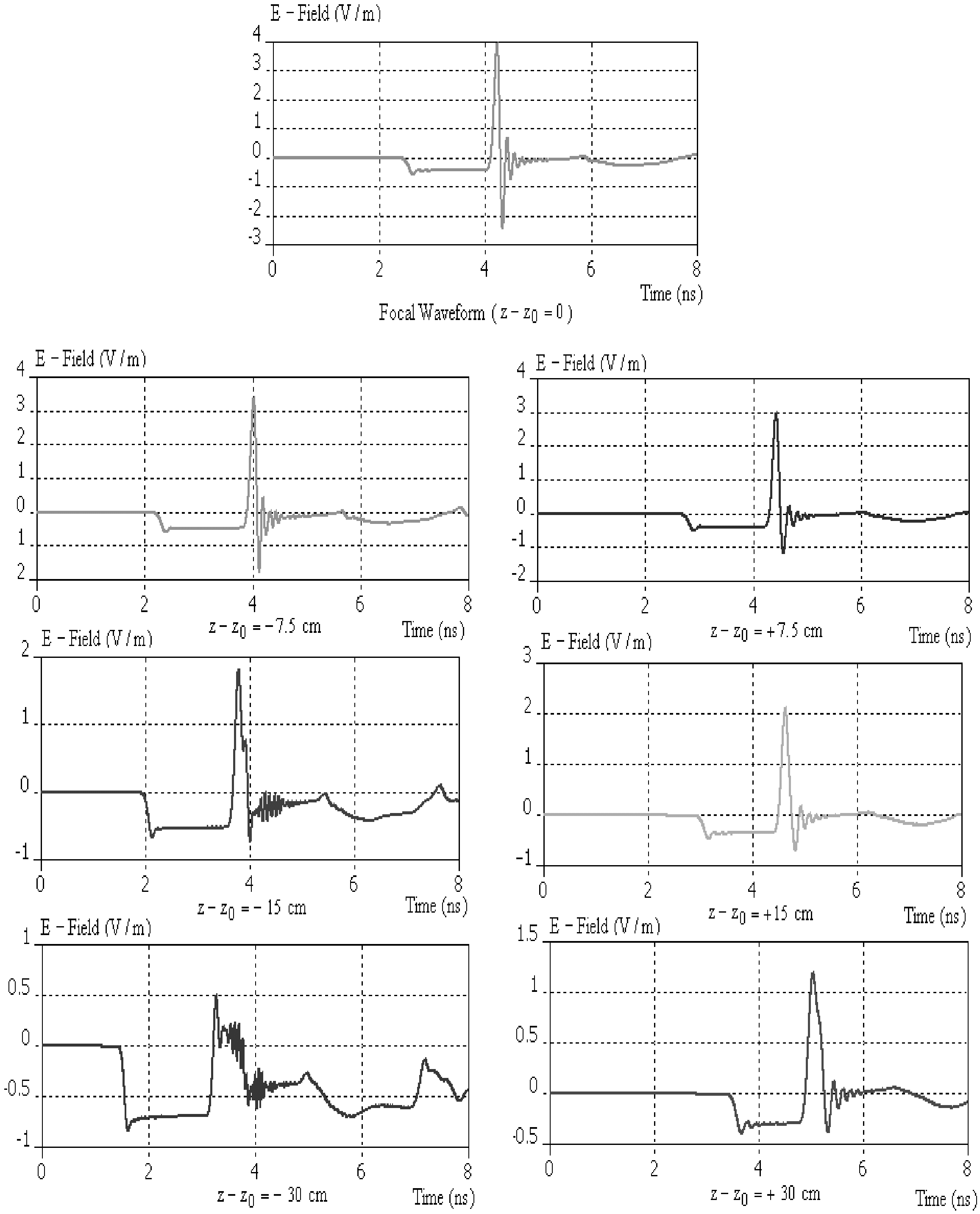

Figure 3.3 Numerical Waveforms wrt z-axis Variations

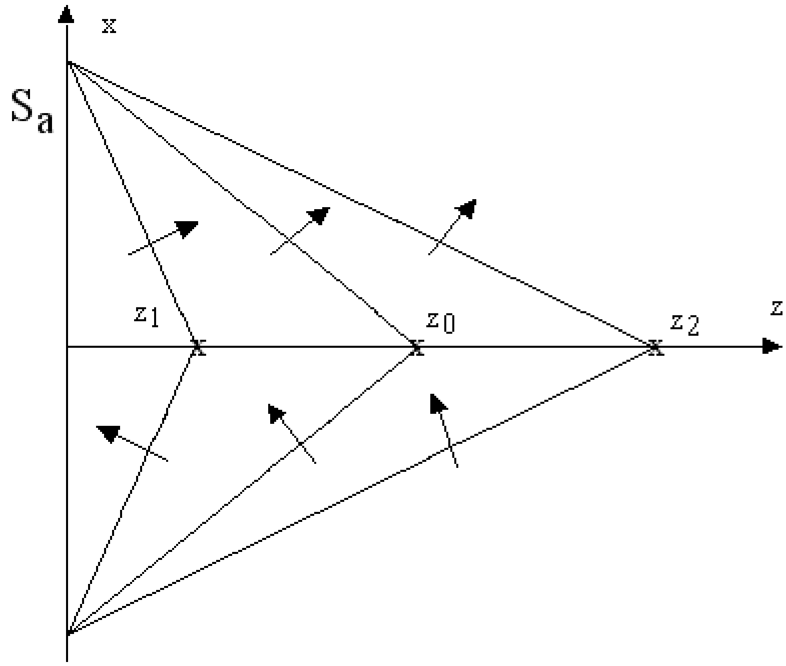

Figure 3.4 E-Field s for different rays

We can see that the waveforms are not symmetrical wrt $z = z_0$ plane (which is not a symmetry plane). We have competing factors. As we move away from S_a this gives lower fields, due to inverse distance in the integrals. However the wave from S_a is not oriented in the x-direction, but is tilted , this being more severe closer to S_a .

3.2 Numerical Waveforms for 45^{o} 4-TEM-Feed-Arm

3.2.1 Numerical waveforms for 45^{o} 4-TEM-feed-arm wrt x-axis variation

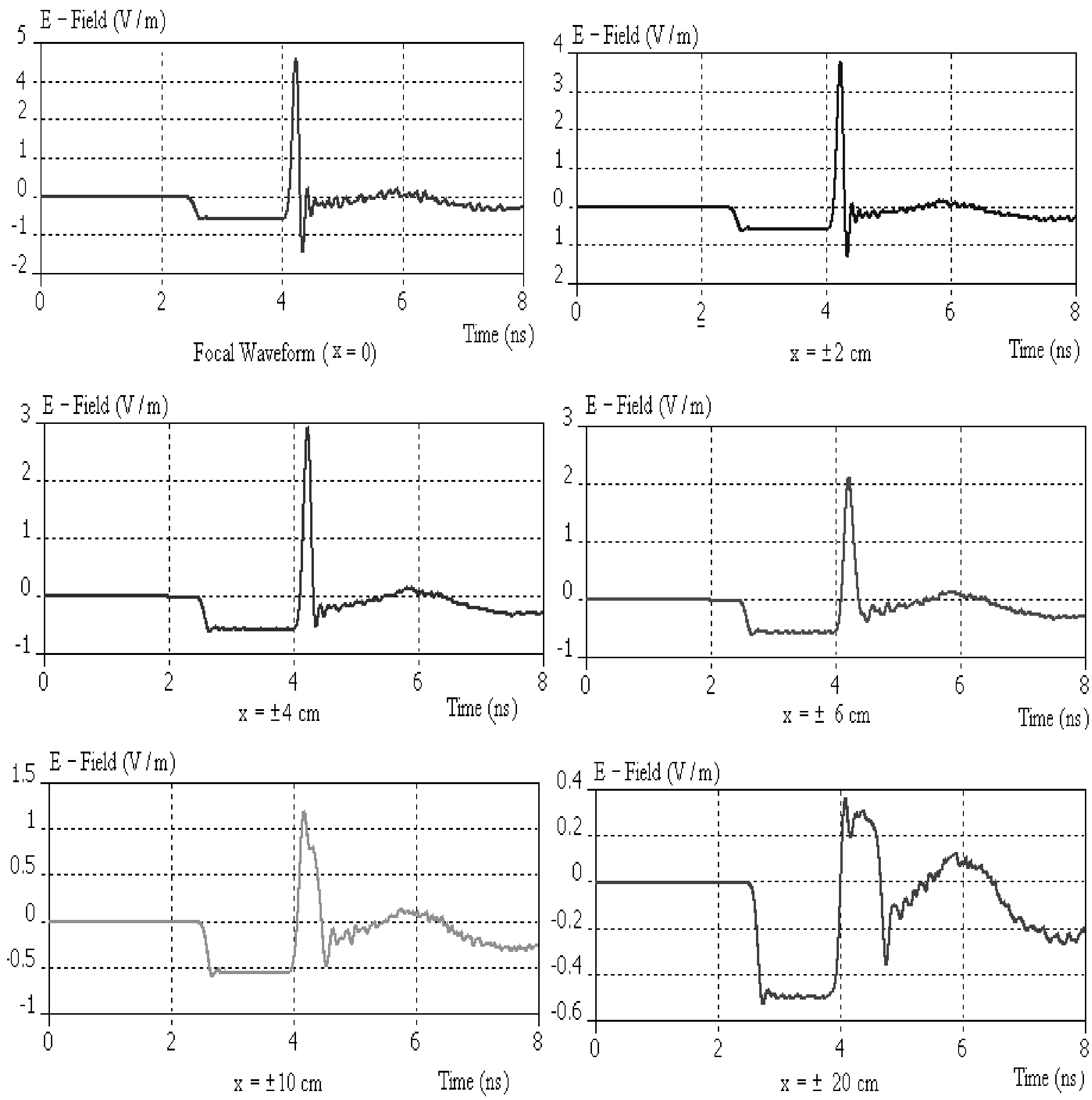

Figure 3.4 Numerical Waveforms wrt x-axis Variations

We do not have any feed arms on the $y = 0$ plane, as we go up in x-axis we are not getting as much amplitude near a feed arm.

3.2.2 Numerical waveforms for 45^{o} 4-TEM-feed-arms wrt y-axis variation

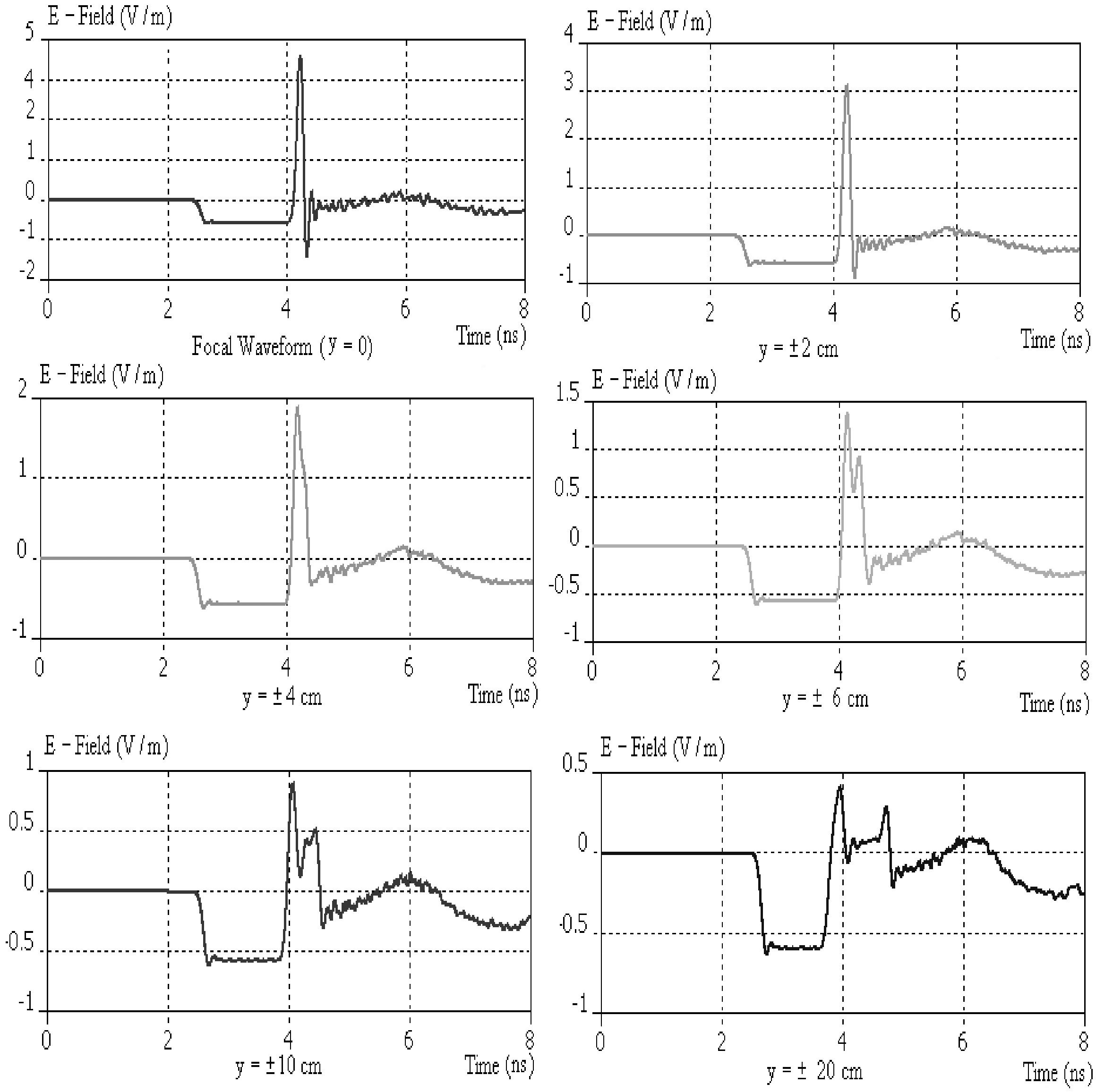

Figure 3.5 Numerical Waveforms wrt y-axis Variations

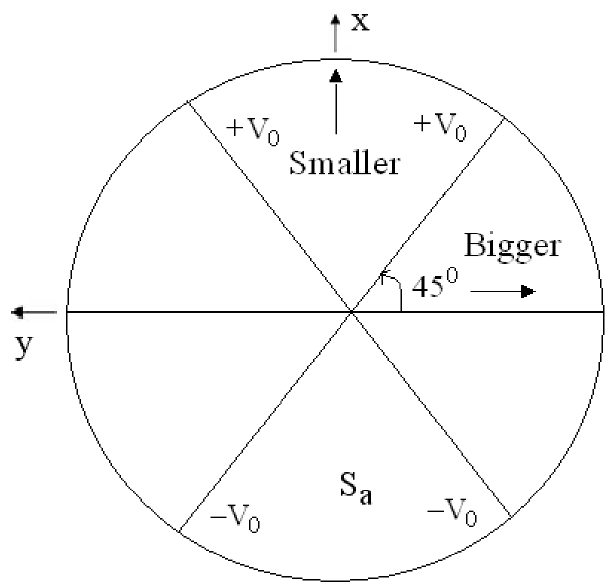

Figure 3.6 E-Field Amplitude Variation for 45^{o} 4-TEM-Feed-Arm

As one can see from Fig 3.4 and Fig 3.5 we are obtaining bigger amplitude for $\pm y$ instead of moving $\pm x$. This result is expected because if we are moving in the x-direction we are having the same charged feed arms on both sides so they are canceling E-fields, whereas moving in the $\pm y$ directions brings us closer to the feed arms with opposite potentials. This is illustrated in Fig. 3.6.

3.2.3 Numerical waveforms for 45^{o} 4-TEM-feed-arms wrt z -axis variation

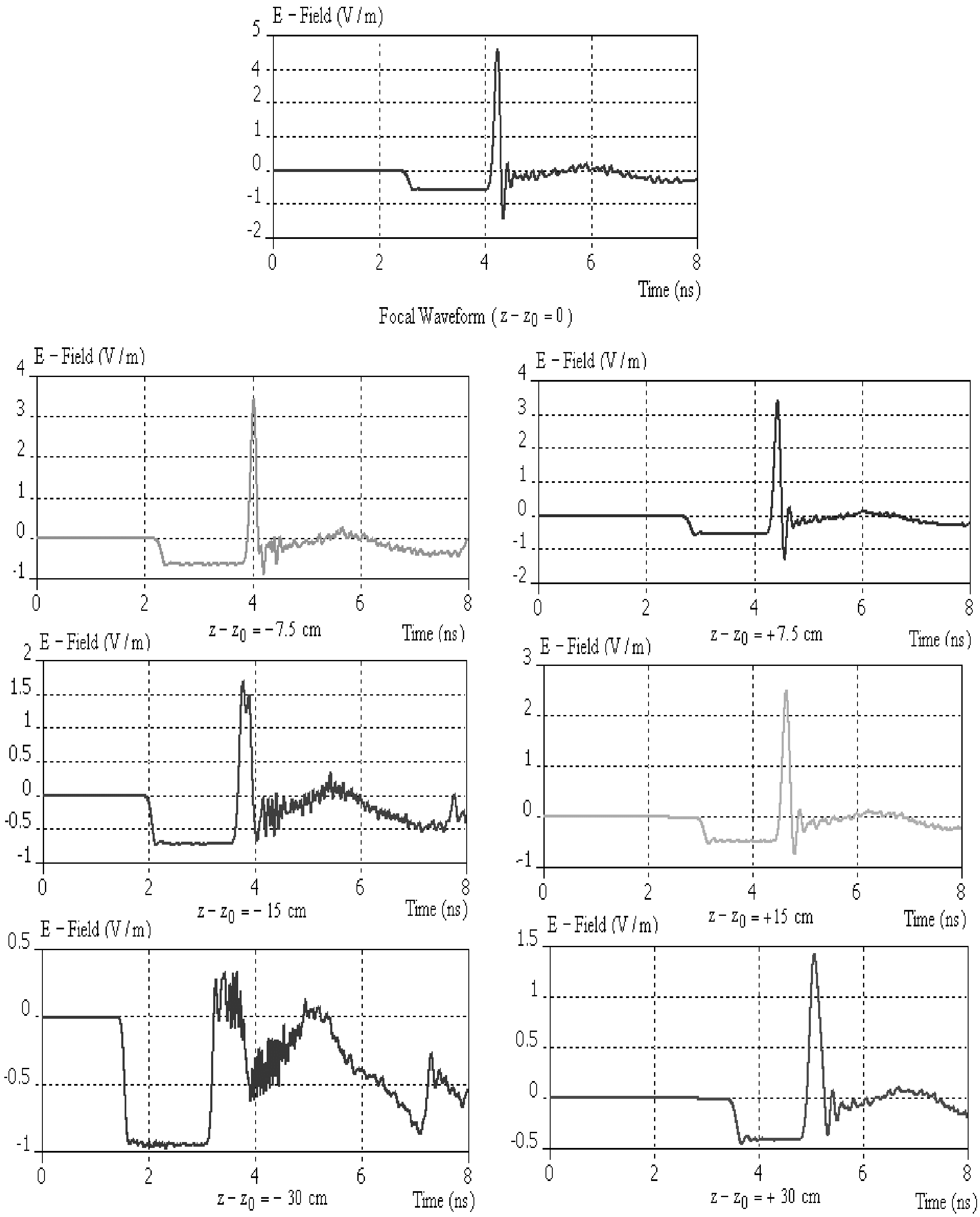

Figure 3.7 Numerical Waveforms 45^{o} 4-TEM-Feed-Arm wrt z-axis Variations

We are getting exactly the same as the 2-arm case with $\sqrt{2}$, except that some numerical errors give differences from the ideal.

3.3 Numerical waveforms for 60^{o} 4-TEM-feed-arm

3.3.1 Numerical waveforms for 60^{o} 4-TEM-feed-arm wrt x-axis

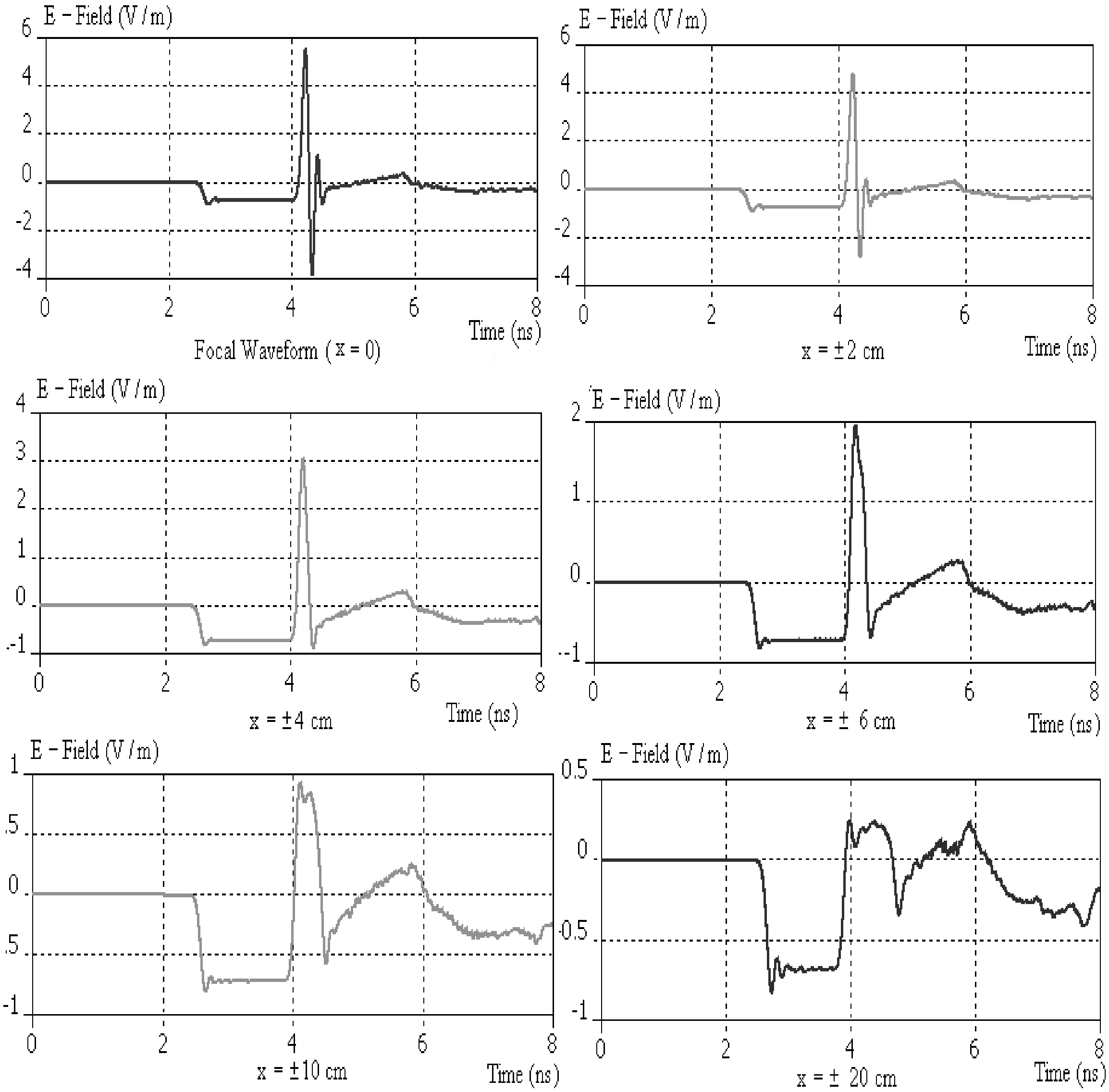

Figure 3.8 Numerical Waveforms wrt x-axis Variations

Around $x = \pm 5\,\text{cm}$ we are getting half of the focal waveform amplitude. One can say $x = \pm 5\,\text{cm}$ is the spot size for x-axis variation.

3.3.2 Numerical waveforms for 60^{o} 4-TEM-feed-arm wrt y-axis

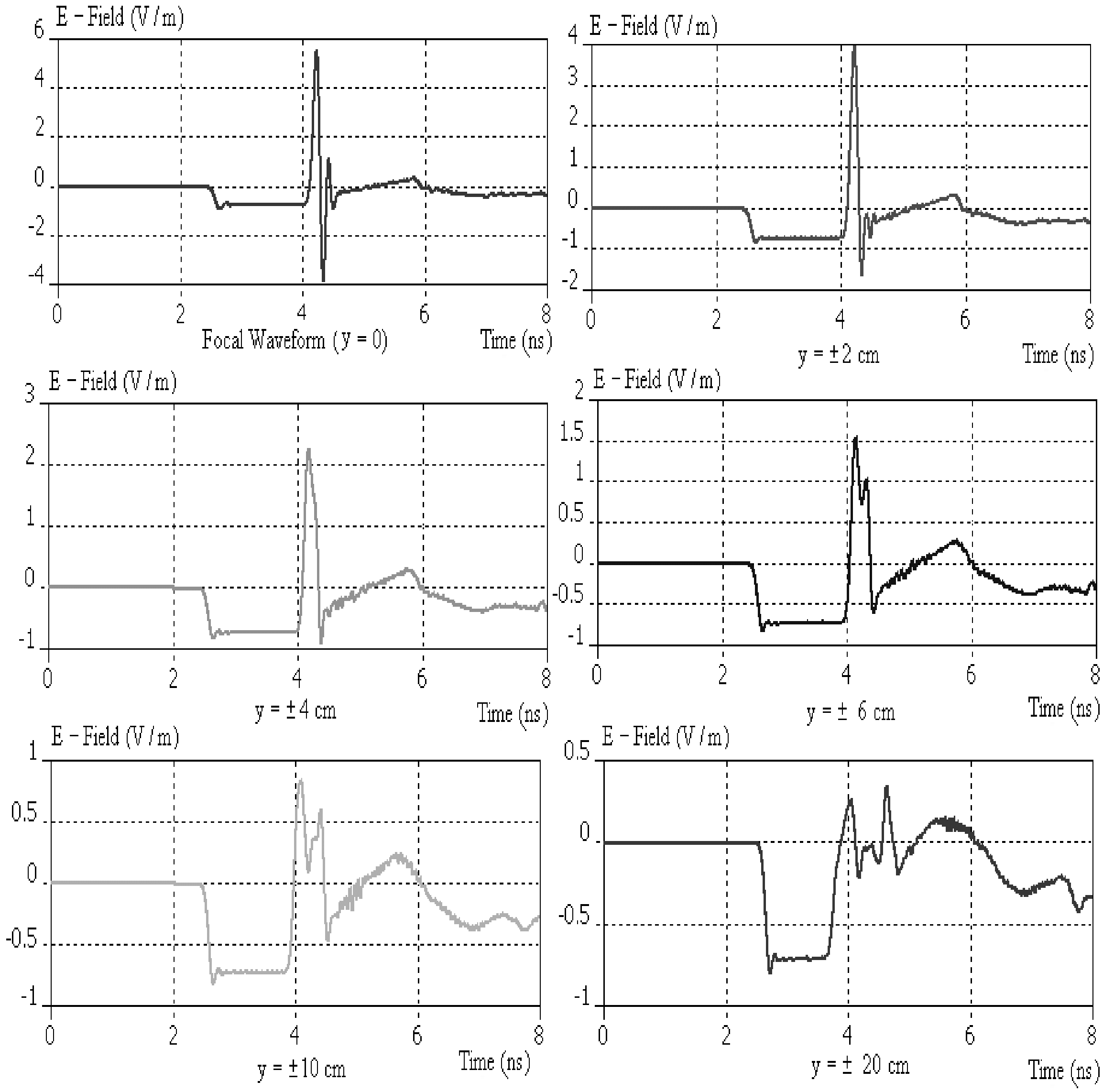

Figure 3.9 Numerical Waveforms wrt y-axis Variations

For the 60^{o} 4-arm case we having more field for x away from zero than for y away from zero. So that means the feed arms fields do not cancel them out that much.

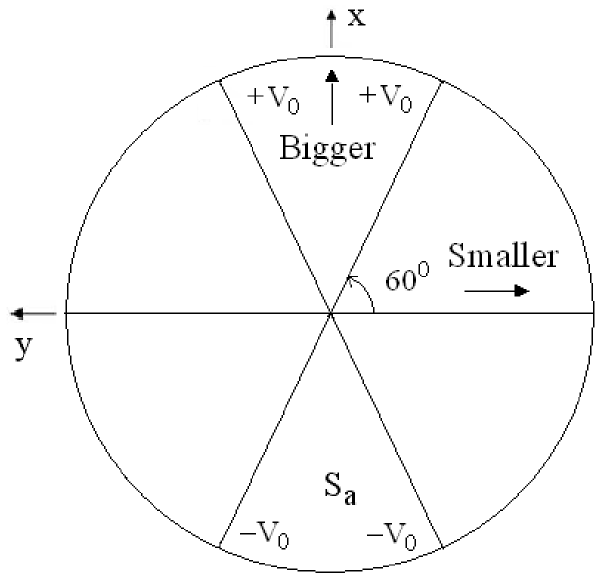

Figure 3.11 E-Field Amplitude Variation for 60^{o} 4-TEM-Feed-Arm

As one can see from Fig 3.8 and Fig 3.9 we are obtaining bigger amplitude for $\pm$ x instead of moving $\pm$ y. This result is expected because if we are moving in the y-direction we are moving away from the feed arms. This is illustrated in Fig. 3.11.

3.3.3 Numerical Waveforms for 60^{o} 4-TEM-Feed-Arm wrt z-Axis

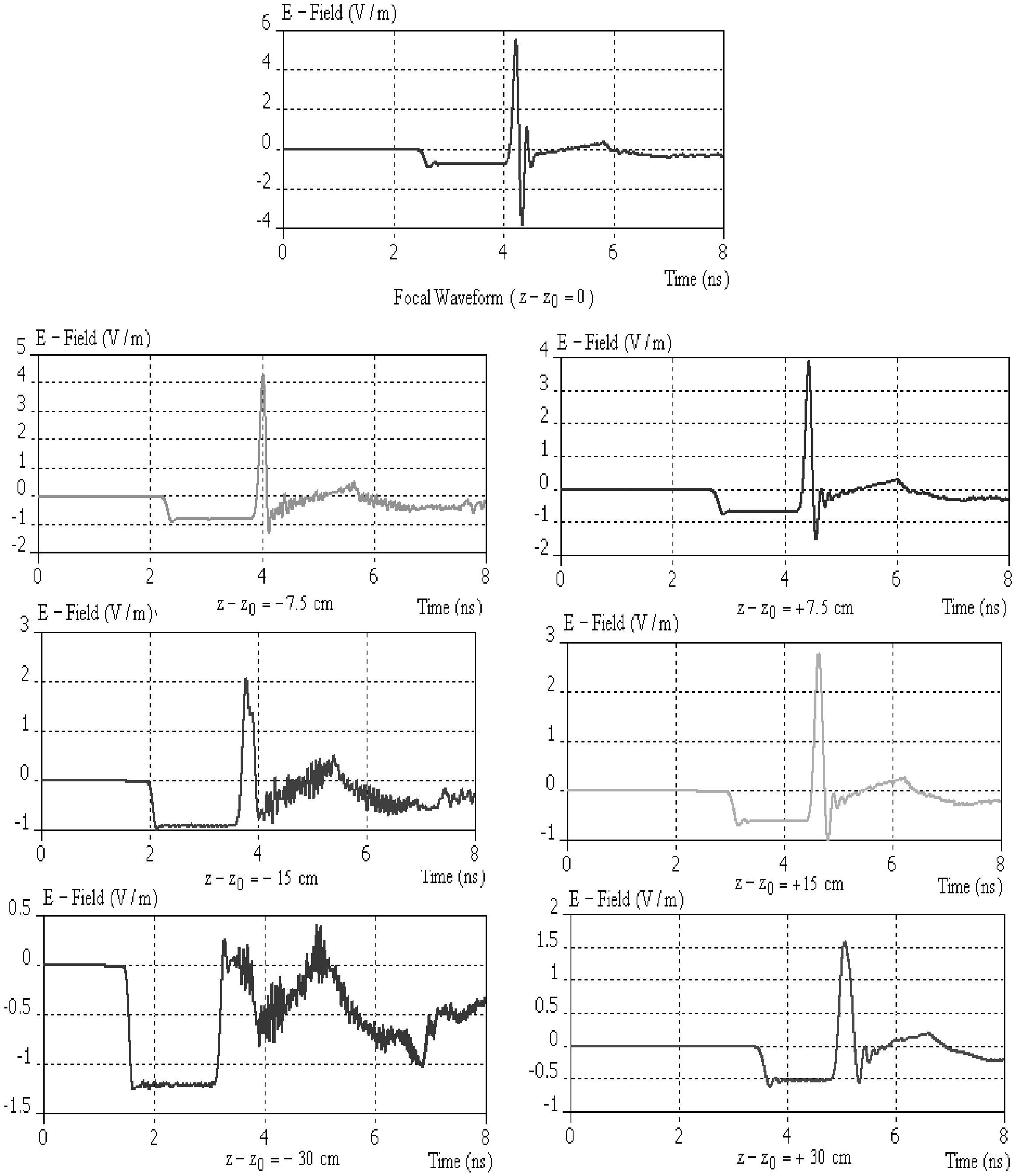

Figure 3.10 Numerical Waveforms wrt z-axis Variations

We can see the same effect as we observed before the wave from S_a is not oriented in the x-direction , but is tilted , this being more severe closer to S_a . We are getting 1.6 times bigger amplitude for waveforms than the 2-arm case, as calculated in [1]. We obtain maximum field uniformity near the origin for the 60^{o} case, in the two-dimensional approximation [4]. However, there are some differences here due to the fact that the wave is not planar.

6.Conclusion

Numerical results for the prepulse term are basically the same as the analytical results. In general the impulse term is approaching the analytic one from below. But especially for the postpulse the numerical computation is inadequate, perhaps due to mesh size and frequency limitations .

The 4-arm case numerical calculations do not improve over the 2-arm case as much as the analytic results would indicate. We attribute this to numerical problems.

References

1. S. Altunc and C. E. Baum, "Extension of the Analytic Results for the Focal Waveform of a Two-Arm Prolate-Spheroidal Impulse-Radiating Antenna (IRA)", Sensor and Simulation Note 518, Nov 2006.
2. S. Altunc and C. E. Baum, "Comparison of Analytical and Numerical Results for a Prolate-Spheroidal Impulse-Radiating Antenna (IRA)", Sensor and Simulation Note 519, Nov 2006.
3. C. E. Baum, "Focal Waveform of a Prolate-Spheroidal IRA", Sensor and Simulation Note 509, February 2006.
4. C. E. Baum, "Impedances and Field Distributions for Symmetrical Two Wire and Four Wire Transmission Line Simulators ", Sensor and Simulation Note 27, Oct 1966.